NUMERICAL CALCULATION OF THERMAL PROCESSES IN CENTRIFUGAL PLASMA POWDER CLADDING

A.I. SOM[1] and **A.T. ZELNICHENKO**[2]

[1]Plasma-Master Ltd., Kiev, Ukraine

[2]E.O. Paton Electric Welding Institute, NASU, Kiev, Ukraine

In this work, thermal processes running in the thick-walled pipe wall at centrifugal plasma powder cladding were studied by computational experiment method. Temperature fields in each point of the item were calculated, depending on the cladding mode. A measuring stand and procedure for determination of the heat transfer coefficient and effective thermal power were developed.

Centrifugal plasma powder cladding (CPPC) is an efficient technological process of deposition of wear-resistant, corrosion-resistant and antifriction coatings on the surface of various parts [1, 2], including the inner surface of cylindrical parts [3]. CPPC (Figures 1 and 2) is conducted by melting a layer of filler powder by transferred plasma arc at fast rotation of the part (500−1200 rpm). A liquid circular pool forms, which moves together with the plasmatron along the part axis. Presence of a circular pool is a mandatory condition of formation of a metal bond between the deposited metal and substrate. Temperature on the part inner surface in the area of pool location should not be lower than the melting temperature of the filler powder. Its overheating is undesirable, as it leads to base metal dissolution and, as a result, to its mixing with the deposited metal.

Provision of optimum cladding conditions depends on mode parameters, primarily, on arc current and plasmatron movement speed. Diameter of the cylindrical part, its wall thickness and thermophysical properties of base metal, also have a great role. In connection with the fact that visual inspection of the

processes of heating, melting and solidification of the filler metal is difficult, selection of optimum mode parameters is highly labour-consuming and costly. Preparation of microsections requires cladding and then cutting several samples of the bushings.

In this work, the method of computational experiment was used to search for optimum CPPC modes. This method was used to study the thermal processes running in the thick-walled pipe wall. Coefficients of heat transfer and effective thermal power required for the computational experiment, were determined using the proposed calculation-experimental method and specially designed measuring stand.

Thermal processes running at CPPC of thick-walled pipes (Figure 3), are described by differential equation of thermal conductivity:

$$c\rho \frac{\partial T}{\partial t} = \frac{1}{r} \frac{\partial}{\partial r}\left(r\lambda \frac{\partial T}{\partial r}\right) + \frac{\partial}{\partial z}\left(\lambda \frac{\partial T}{\partial z}\right), \qquad (1)$$

$$R_{in} < r < R_o, \quad 0 < z < H,$$

where c, ρ, λ is the specific heat capacity, density and coefficient of material heat conductivity; T is the temperature; r, z are the radial and axial coordinates; t is the time; R_{in}, R_o are the pipe inner and outer radius; H is the pipe length.
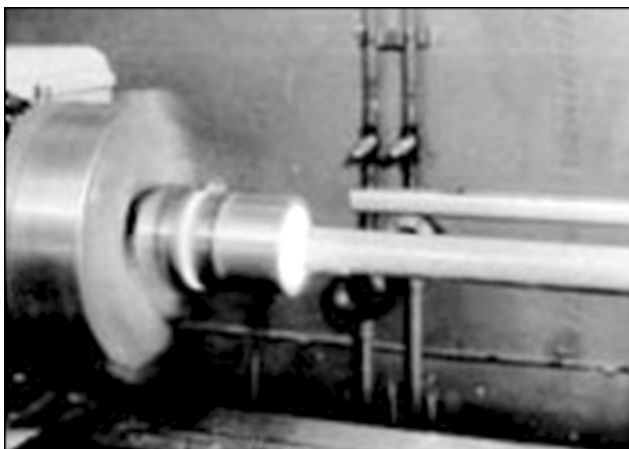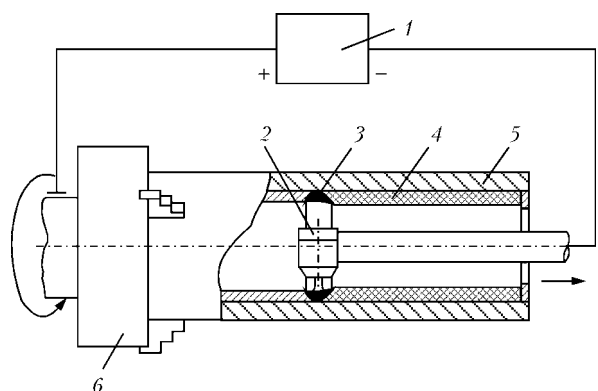

Figure 1. Fragment of a machine for CPPC performance

Figure 2. Schematic of the process of CPPC on the part inner surface [1]: *1* — power source; *2* — plasmatron; *3* — circular weld pool; *4* — filler powder; *5* — part; *6* — chuck
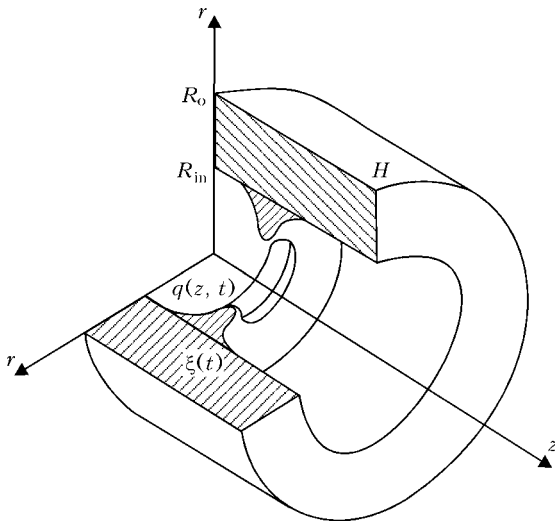
Figure 3. Schematic of bushing heating accepted for calculations

Let us assume that the heat source, moving in the axial direction along the inner surface of rapidly wearing pipe, is distributed by the normal law:

$$q(z, t) = q_0 \exp\left[-k(z - \xi(t)^2)\right], \qquad (2)$$

where q_0 is the maximum density of the heat flow; k is the concentration coefficient; $\xi(t)$ is the current co-ordinate of the source:

$$\xi(t) = \begin{cases} t_0, & t < t_{in}; \\ t_0 + vt, & t > t_{in}, \end{cases}$$

where t_{in} is the duration of arc impact in the initial point with co-ordinate z_0; v is the speed of source movement.

Total power of heat source Q is connected to value q_0 by the following ratio:

$$q_0 = \frac{Q\sqrt{k/\pi}}{2\pi R_{in}}. \qquad (3)$$

Processes of heat transfer and radiation exchange with the environment run on the outer and end face surfaces of the pipe, environment temperature T_{en} being expressed as

$$-\lambda \frac{\partial T}{\partial r}\bigg|_{r = R_o} = \alpha_2(T - T_{en}) + \varepsilon\delta(T^4 - T_{en}^4) \qquad (4)$$

or

$$-\lambda \frac{\partial T}{\partial r}\bigg|_{r = R_o} = \alpha'_2(T - T_{en}), \qquad (5)$$

where

$$\alpha'_2 = \alpha_2 + \varepsilon\sigma(T - T_{en})(T^4 - T_{en}^4). \qquad (6)$$

Similarly,

$$-\lambda \frac{\partial T}{\partial r}\bigg|_{z = 0} = \alpha'_3(T - T_{en}), \qquad (7)$$

$$-\lambda \frac{\partial T}{\partial r}\bigg|_{z = H} = \alpha'_1(T - T_{en}), \qquad (8)$$

where α is the coefficient of heat transfer; ε is the emissivity factor; δ is the Stefan–Boltzmann constant.

In addition to the above-mentioned processes, transfer of heat source energy occurs on the pipe inner surface. Part of this energy is consumed in heating and melting of filler powder. Simulation of the process of powder heating at plasma powder cladding was performed in [4]. In keeping with study [5] the powder layer can be presented in the form of concentrated heat capacity. In this case, the boundary condition on the pipe inner surface has the following form:

$$\lambda \frac{\partial T}{\partial r}\bigg|_{r = R_{in}} = q(z, t) + \alpha'_4(T - T'_{en}) + C_p \frac{\partial T}{\partial t}\bigg|_{r = R_{in}}, \qquad (9)$$

where C_p is the heat capacity of the deposited powder layer equal to ρcS; S is the powder layer thickness.

Equation (1) with boundary conditions (4), (5), (7), (8) was solved* by the method of finite differences (taking into account temperature dependence of heat capacity and thermal diffusivity of bushing material). Integration of a two-dimensional equation of heat conductivity was reduced to solving two one-dimensional problems in keeping with local one-dimensional schematic of A.A. Samarsky [6] and procedure of allowing for concentrated heat capacity proposed in work [5].

Proceeding from the developed models and computational algorithm software has been developed, envisaging on-line entry of initial data and graphic representation of results in the form of isotherms and thermal cycles in assigned points. Values of heat transfer coefficient α and effective thermal power q, required for practical calculations, were determined experimentally.

It is known that heat transfer coefficient depends on the shape and dimensions of the surface releasing the heat, its position in space, properties of the environment and other factors. Therefore, experiments on its determination were conducted under the conditions maximum close to the real conditions.

The essence of measurement procedure consisted in the following. A cylinder of steel 20 of 80 mm diameter and 300 mm length was heated in the furnace up to the temperature of 900 °C, mounted in the lathe centers, made to rotate at the speed of 800 rmp and an optical pyrometer was used to record the curves of cylindrical surface cooling (thermally insulating inserts were mounted on cylinder end faces to eliminate heat transfer). Cylinder cooling process was also simulated in the computer. For this purpose equation (1) was solved with the following boundary conditions:

---

*A.V. Romanenko participated in numerical integration.

$$\lambda \frac{\partial T}{\partial r}\Big|_{r=0} - \lambda \frac{\partial T}{\partial r}\Big|_{r=R_o} = \alpha(T - T_{en}) + \varepsilon\sigma(T^4 - T_{en}^4).$$

A series of calculations were performed with different α values, the results of which were compared with experimental data. For further calculations of thermal processes, value $\alpha = 50$ W/(m^2·K) was selected, at which the calculated curve was the closest to the experimental one.

As is seen from Figure 4, a slight discrepancy between the experimental and calculated cooling curves of the studied cylinder in the temperature field of 500−700 °C is associated with running of phase transformations in steel, which are not allowed for in model (1)−(9).

Energy characteristics of the plasma arc have been quite well studied for the case of welding, cutting and surfacing [7−10]. However, the results of this work cannot be used for evaluation of effective thermal power of the arc at centrifugal cladding, as item heating in this case has significant special features: the arc runs in a closed space and moves relative to the heated surface at the speed of 3−5 m/s, i.e. by 2−3 orders of magnitude higher than with other plasma processing methods. It should be also taken into account that the effective arc efficiency depends essentially on plasmatron design and its operation mode.

Effective thermal power of the arc was determined by calorimetry, using a thick-walled copper sleeve of 7900 g mass with 80 mm inner diameter and 100 mm length of the cylindrical section as the calorimetric body. The sleeve had a stainless steel stem brazed to its bottom for its fastening in the machine chuck, as well as a case with thermal insulation from basalt fiber. A connector for connection of an external measuring system to two chromel-copel thermocouples caulked into the sleeve, is mounted into the case. The essence of the procedure of determination of the arc effective thermal power was reduced to measurement of the amount of heat, which was gained by the calorimetric body per a unit of arcing time:

$$q_e = \frac{Q_b}{t_r} = \frac{C_{cop}m\Delta T}{t_r},$$

where C_{cop} is the specific heat capacity of copper; m is the calorimetric body weight; ΔT is the temperature increment; t_r is the arc revolution time.

Body temperature was recorded by three-point potentiometer KSP-4 cl. 0.5 with 0−100 °C scale. Arcing time was assigned using the electronic timer, and it was recorded with digital millisecond meter F.291, the signal to which came from current sensor. The signal of arc ignition simultaneously came to the potentiometer. Arc current and voltage were recorded using instruments of magnetoelectric system of cl. 0.2. Experiments were conducted in UD251 unit (Figure 5). A plasmatron with a tungsten electrode was used in the experiments. Plasmatron nozzle diameter
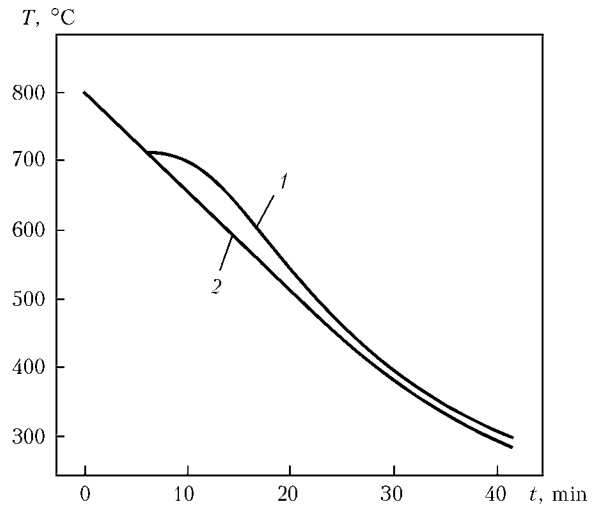

Figure 4. Experimental (*1*) and calculated (*2*) curves of cooling of a cylinder of 80 mm diameter at revolution with the speed of 800 rpm ($\alpha = 50$ W/(m^2·K))

was 5 mm, nozzle length was 5 mm, depth of electrode immersion into the nozzle was 5 mm, and plasma gas was argon.

Arc parameters were varied within the following ranges: arc current of 300−700 A; arc length of 5−15 mm; plasma gas consumption of 4−20 l/min; calorimeter revolution speed of 50−1250 rpm. When changing one parameter, the others were kept constant and close to optimum ones.

Experimental sequence was as follows. Plasmatron was inserted into the calorimetric body cavity, potentiometer was connected and initial calorimeter curve was recorded. Then, the potentiometer was disconnected, without switching off diagram tape feed to record the moment of arc striking, calorimeter rotation was switched on and the arc was excited. After 6−8 s the arc was switched off, the calorimeter was stopped, the plasmatron was quickly taken out of it and the cover was put on. Potentiometer was simultaneously
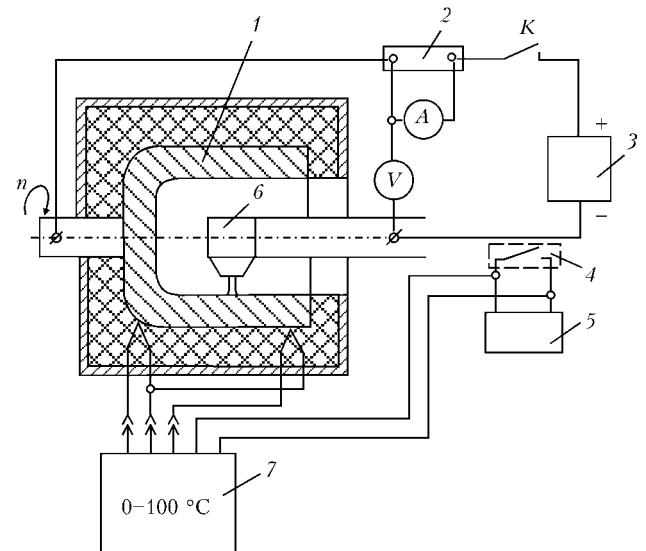

Figure 5. Schematic of UD251 unit for determination of effective thermal power of the arc: *1* — calorimeter; *2* — shunt; *3* — welding rectifier; *4* — current sensor; *5* — millisecond meter; *6* — plasmatron; *7* — potentiometer
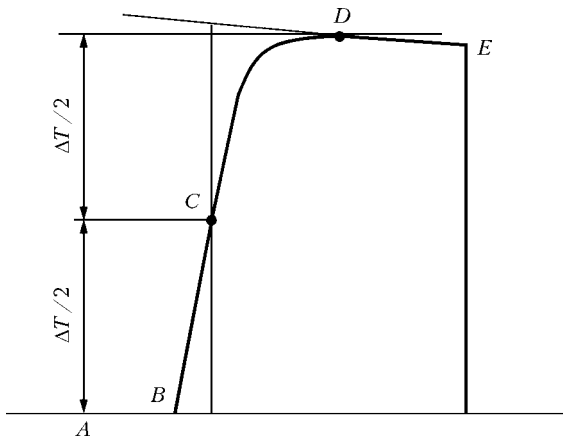
SCIENTIFIC AND TECHNICAL

Figure 6. Full cycle of calorimeter temperature variation: *AB* — initial period; *BCD* — main period; *DE* — final period

Figure 8. Dependence of arc voltage on cladding current (Q_{melt} = = 10 l/min; n = 800 rpm) at arc length L_a = 15 (*1*), 10 (*2*) and 5 (*3*) mm

connected and the main and final periods of calorimeter temperature curve were recorded. Figure 6 gives an example of recording the full cycle of calorimeter temperature change. Before conducting the next experiment, the calorimeter was cooled to room temperature by an air jet.

Calorimeter heat losses into the environment because of imperfect thermal insulation were allowed for through a correction for heat exchange, which was graphically determined in each experiment by a procedure described in [10]. The actual temperature value, allowing for this correction, was found by extrapolation of the initial and final temperature change
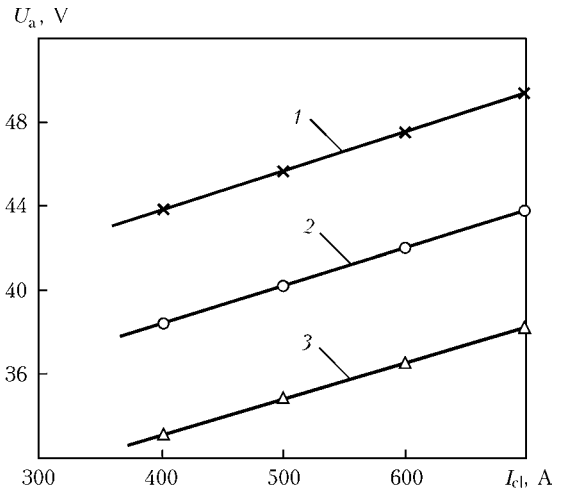
by straight lines up to the moment of the main period, when system temperature change will amount to half of the observed change (point *C*). Each experiment was repeated 3–4 times. Some investigation results are given in Figures 7 and 8.

To check the adequacy of the calculation model, heating of outer surface of steel bushing during cladding (bushing inner diameter of 105 mm, outer diameter of 135 mm, length of 250 mm) was experimentally studied. Powder of PG-SR4 grade (GOST 21448–75) with 80–200 μm particle size was used as
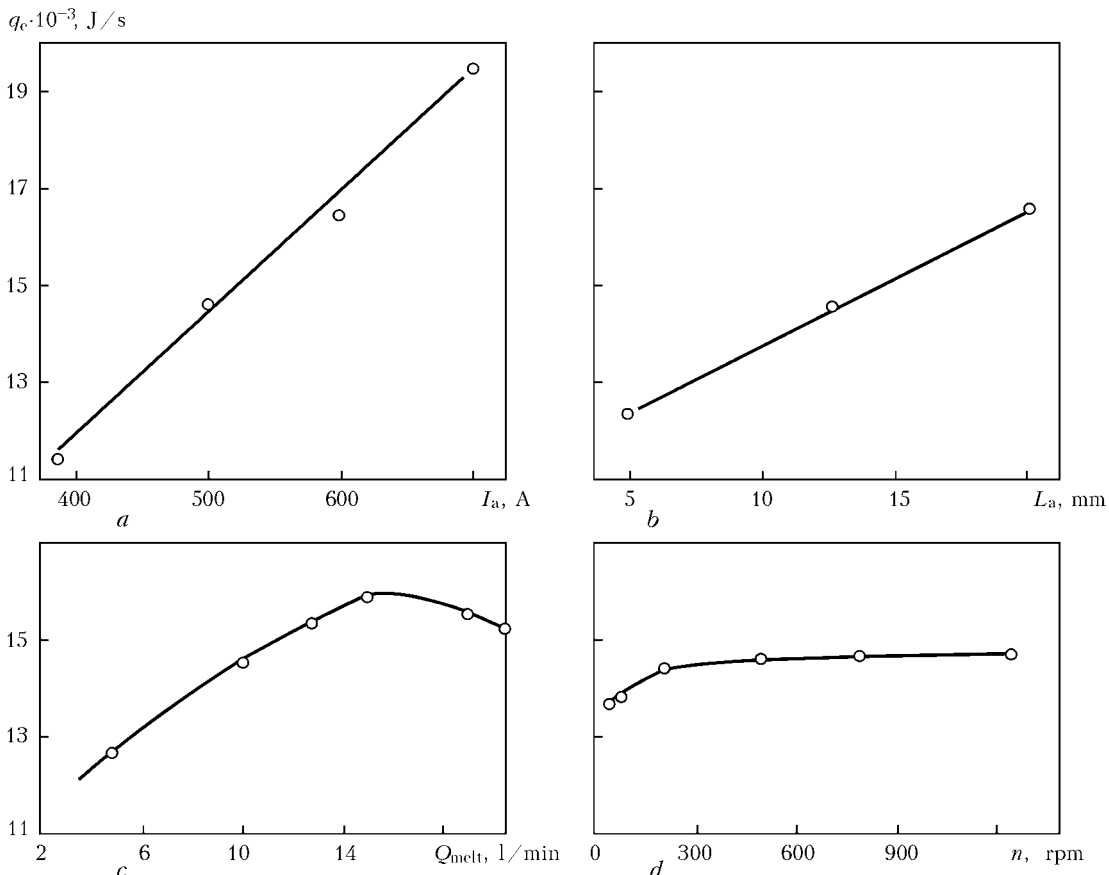

Figure 7. Dependence of effective thermal power of plasma arc on current (*a*), arc length (*b*), plasma gas consumption (*c*) and arc rotation speed (*d*) at Q_{melt} = 10 l/min (*a, b, d*); L_a = 10 mm (*a, c, d*); n = 800 rpm (*a–c*); I_a = 500 A (*b–d*)
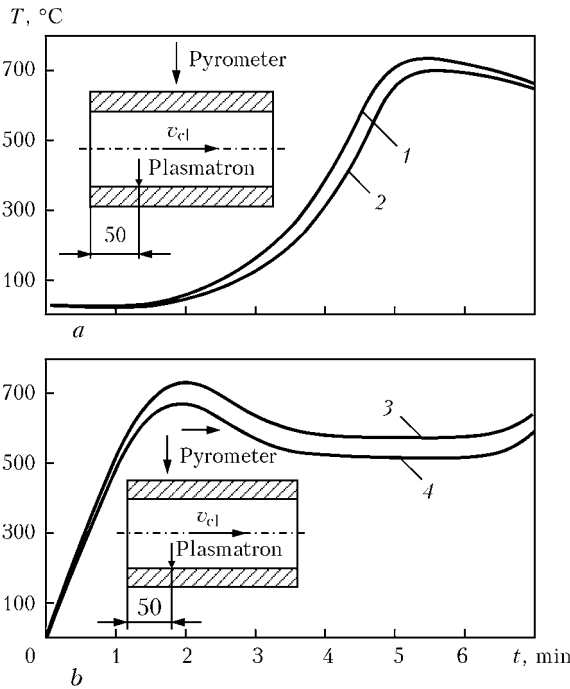
a

b

Figure 9. Change of temperature of busing outer surface during cladding in mid-section (*a*) and in sections coinciding with arc axis (*b*): *1, 3* — calculated curves; *2, 4* — experimental curves

Figure 10. Thermal field (°C) in the wall of bushing of drill pump UNBT-950 8 min after the start of cladding

filler material. Cladding mode was as follows: arc current of 500 A, speed of plasmatron axial movement of 35.5 mm/min, plasma gas (argon) flow rate of 10 l/min, part rotation speed of 800 rpm, and deposited layer thickness of 2 mm. Cladding was started at 50 mm distance from the bushing left end. The main criteria for selection of cladding mode parameters were good formation of the deposited layer and minimum penetration of base metal (< 3 %).

Temperature was recorded at stationary pyrometer aimed at the bushing middle (Figure 9, *a*) and at its displacement along the bushing in synchronism with the arc (Figure 9, *b*). In the latter case, the pyrometer optical axis and plasmatron axis coincided. Maximum discrepancy of experimental and calculated curves is not more than 7 %.

The developed mathematical model allows calculation of temperatures in any point of the item, depending on cladding mode, thus essentially facilitating selection of optimum mode parameters. For instance, having assigned the temperature of the bushing wall inner surface, it is possible to select the effective thermal power of the arc, speed of plasmatron axial displacement and other mode parameters, ensuring this temperature by successive approximation method (this problem is solved in 10—15 min in the PC). Software allows tracing on the computer monitor the item thermal state at any moment of cladding, which is highly important for the non-stationary process (start and end of cladding, cladding of bushings with variable wall thickness, etc.).

Figure 10 shows as an example the thermal field of a bushing of UNBT-950 drill pump 8 min after the start of cladding. Bushing dimensions are as follows:
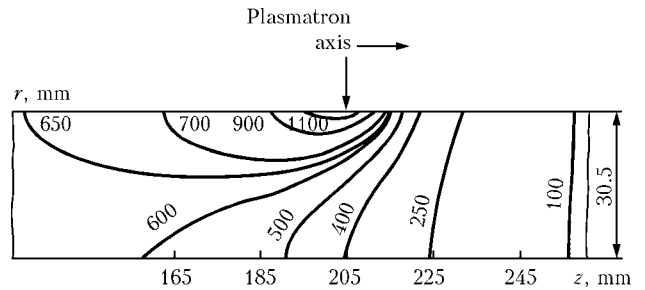
inner diameter of 154 mm, outer diameter of 215 mm, length of 450 mm. Cladding mode was as follows: arc current of 2 × 600 A; speed of plasmatron axial displacement of 30 mm/min; plasma gas flow rate in each plasmatron of 10 l/min; arc length of 10 mm; thickness of deposited layer of 2.5 mm: speed of part rotation of 800 rpm. Cladding started at 50 mm distance from the bushing left end face. Deposited material was iron-based alloy. Figure 11 shows temperature change on the wall inner and outer surface for the same bushing during the entire cladding cycle. Analysis of the given curves shows that this cladding mode is close to the optimal one. Temperature on the bushing inner wall at the steady-state process is equal to 1240 °C, which is by 100—150 °C higher than the filler powder melting temperature, and, therefore, fu-
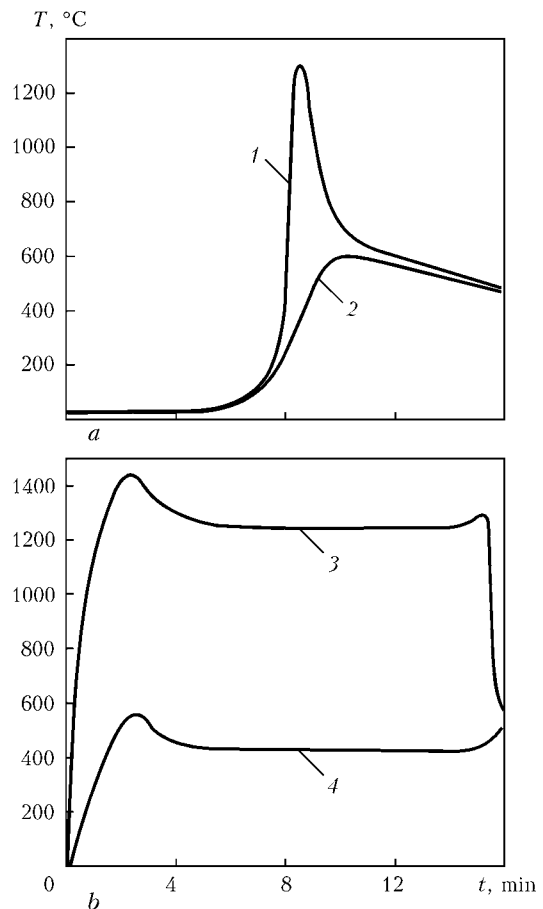

a

b

Figure 11. Change of temperature on inner (*1, 3*) and outer (*2, 4*) surfaces of bushing wall in mid-section (*a*) and in sections coinciding with arc axis (*b*)

Figure 12. Transverse macrosection of bushing

sion of the deposited layer with base metal should be ensured. On the other hand, it is lower than base metal melting temperature, so that deposited metal dilution should be minimum. Figure 12 shows a transverse macrosection of the bushing, which confirms the drawn conclusion.

CONCLUSIONS

1. Developed mathematical model of item heating at CPPC quite accurately describes the thermal processes. Conducted series of computational experiments allowed optimization of cladding parameters.

2. Calculation-experimental procedure of determination of the coefficient of heat transfer from the surface of the rotating bushing allowed determination of its value, which is equal to 50 W/(m^2·K).

3. Measuring stand has been developed and a procedure has been proposed for determination of effective heat power at CPPC. Obtained quantitative data have been used with success in engineering calculations.

1. Gladky, P.V., Pereplyotchikov, E.F., Ryabtsev, I.A. (2007) *Plasma cladding*. Kiev: Ekotekhnologiya.
2. Pereplyotchikov, E.F., Ryabtsev, I.A. (2007) *Plasma-powder cladding in armature engineering*. Kiev: Ekotekhnologiya.
3. Gladky, P.V., Som, A.I., Pereplyotchikov, E.F. (1984) Centrifugal plasma cladding. In: *New processes of cladding, properties of deposited metal and transition zone*. Kiev: PWI.
4. Gladky, P.V., Pavlenko, A.V., Zelnichenko, A.T. (1989) Mathematical modeling of powder heating in the arc during plasma cladding. *Avtomatich. Svarka*, **11**, 17–21.
5. Zelnichenko, A.T. (1984) Difference scheme of end-to-end count for equation of heat conductivity with concentrated heat capacity. *Vych. i Prikladn. Matematika*, Issue 53, 57–65.
6. Samarsky, A.A. (1977) *Theory of difference schemes*. Moscow: Nauka.
7. Vajnbojm, D.I., Ratmanova, Zh.V. (1974) Power characteristics of argon arc with different degree of constriction. *Svarochn. Proizvodstvo*, **5**, 1–3.
8. Kulagin, I.D., Nikolaev, A.V. (1960) *Treatment of materials by arc plasma jet*. Moscow: A.A. Bajkov IM.
9. Stikhin, V.A., Patskevich, I.R. (1967) Determination of thermal characteristics of constricted arc. *Svarochn. Proizvodstvo*, **9**, 26–27.
10. Popov, M.M. (1954) *Thermometry and calorimetry*. Moscow: MGU.